COUPLING OF SYSTEM THERMAL-HYDRAULICS AND MONTE-CARLO METHOD FOR A CONSISTENT THERMAL-HYDRAULICS-REACTOR PHYSICS FEEDBACK

BY

XU WU

THESIS

Submitted in partial fulfillment of the requirements
for the degree of Master of Science in Nuclear, Plasma and Radiological Engineering
in the Graduate College of the
University of Illinois at Urbana-Champaign, 2013

Urbana, Illinois

Master's Committee:

Assistant Professor Tomasz Kozlowski, Chair
Professor Rizwan Uddin

Abstract

The present thesis describes the coupling of a three-dimensional continuous-energy Monte Carlo reactor physics code, Serpent, with thermal-hydraulics safety analysis code RELAP5-3D. Thermal-hydraulics and reactor physics coupling is commonly used in deterministic methods, for example RELAP5/PARCS and TRACE/PARCS. It has been well-validated for a number of steady and transient problems. The coupling of Monte-Carlo and reactor thermal-hydraulics will significantly improve the MC predictive capability and its applicability to a wide range of reactor problems of practical interest, as right now it is limited to fixed-feedback conditions.

In this thesis, the coupled Serpent/RELAP5-3D code capability is demonstrated by the improved axial power distribution of single assemblies, achieved by a consistent thermal-hydraulics feedback. The code coupling is demonstrated for the UO2 and MOX single assemblies based on the OECD-NEA/NRC PWR MOX-UO2 Core Transient Benchmark [1]. Comparisons of calculation results using the coupled code with those from the individual codes in stand-alone mode, also with deterministic methods, specifically heterogeneous multi-group transport code DeCART, show that the coupling produces more precise results.

Acknowledgements

I would like to acknowledge the support from many people in the Department of Nuclear, Plasma and Radiological Engineering. My advisor, Dr. Tomasz Kozlowski, who gave me many insights and financial support. He offered so much time, patience and guidance, without which I would not have been able to complete my Master's thesis. Many thanks are due to Idell Dollison, Gail Krueger and Becky Meline, the best staff I have ever met. They were so helpful during my research in the department. I would also like to express my appreciation to Dr. Rizwan Uddin, my thesis reader and Dr. Stubbins, the department head.

Also, I would like to thank my dear friends Rabie Abu Saleem, Rijan Shrestha, Qiyue Lu, Yinbin Miao and Hsingtzu Wu for their encouragement and help during my work. Finally, I would like to thank my family for their love and backing. And my girlfriend, Cong Xu, who always stayed with me during my study and work in this university when I need her help and support.

Xu Wu

Contents

List of Figures

List of Tables

Nomenclature

P	Pressure
U_g	Gas specific internal energy
U_f	Fluid specific internal energy
α_g	Void fraction
v_g	Gas velocity
v_f	Fluid velocity
X_n	Non-condensable quality
ρ_b	Boron density
k_{fuel}	Thermal conductivity of fuel
k_{clad}	Thermal conductivity of clad material
$c_{p,fuel}$	Heat capacity of fuel material
$c_{p,clad}$	Heat capacity of clad material
ρ_{fuel}	Fuel density
ρ_{clad}	Clad density
T	Temperature
$f_{low}(T)$	Atomic fraction of the low temperature isotope
$f_{high}(T)$	Atomic fraction of the high temperature isotope

CHAPTER 1. INTRODUCTION

Numerical simulation of an operating nuclear reactor or its components provides us an effective method to understand the physics and thermal-hydraulics behavior of the system, while relieving us from the high cost of doing experiments. Also, many simulation codes have been developed for a wide range of numerical and physical approximations, verified by numerical benchmarks and validated by experimental tests. To model a reactor core, several levels of fundamental physical processes require detailed consideration. Neutronics processes like neutron transport, cross-section dependence on the energy and temperature, fission power production and deposition. Thermal-hydraulics processes like heat transfer from fuel to coolant (moderator), flow of the coolant and removal of heat from the system.

However, even if we solve the above processes independently, by no means can we separate them if we want to have an accurate understanding of the reactor core. Each of these processes yield solutions which are source terms for another physical process. Moreover, strong feedback exists between them. These reasons force us to find a method by which we can solve the neutron physics and thermal-hydraulics together to obtain important safety parameters like fission power, fuel temperature and coolant density. The term ‘multi-physics’ means the requirements for a coupling of discrete physics. This is fulfilled by coupling neutronics and thermal-hydraulics calculations.

Great efforts have been made in multi-physics research for reactor safety simulation. Researchers have successfully coupled neutronics and thermal-hydraulics codes to analyze fuel assembly and even whole cores. T. Kozlowski [2] coupled three dimensional

neutron kinetics code PARCS with thermal-hydraulics code RELAP5 to perform consistent comparison of the point kinetics and spatial kinetics analysis of the OECD/NEA (Organization for Economic Co-operation and Development / Nuclear Energy Agency) PWR (Pressurized Water Reactor) MSLB (Main Steam Line Break) transient. Y. Xu [3] used coupled TRACE/PARCS codes to analyze OECD LWR (Light Water Reactor) benchmarks and the Advanced CANDU Reactor, the ACR-700.

The idea of code coupling was also applied to more innovative core types. X. Xi [4] coupled Computational Fluid Dynamics (CFD) code CFX and neutronics code MCNP, in the simulation of Generation IV SCWR (Super Critical Water Reactor) fuel assembly. K. Ivanov [5] summarized the challenges in coupled thermal–hydraulics and neutronics simulations for LWR safety analysis. He recommended the adoption of 3-dimensional thermal-hydraulics models coupled with 3-dimensional neutronics models, as well as improving the accuracy and efficiency in coupled methodologies consistently, and integrating more features like fuel management and safety analysis.

The most recent work from D. Walter [6] coupled three independent simulation tools: neutronics code DeCART, coolant and crud chemistry code MAMBA and CFD code STAR-CCM+. This coupling method demonstrated high fidelity simulation of crud deposition, as well as feedbacks between it and other primary physics. This is a new direction in the code coupling, where the efforts are not limited to just neutronics and thermal-hydraulics. Other features like chemistry or mechanical issues can be implemented into coupling. The Figure 1.1 shows the information exchange among the three codes.

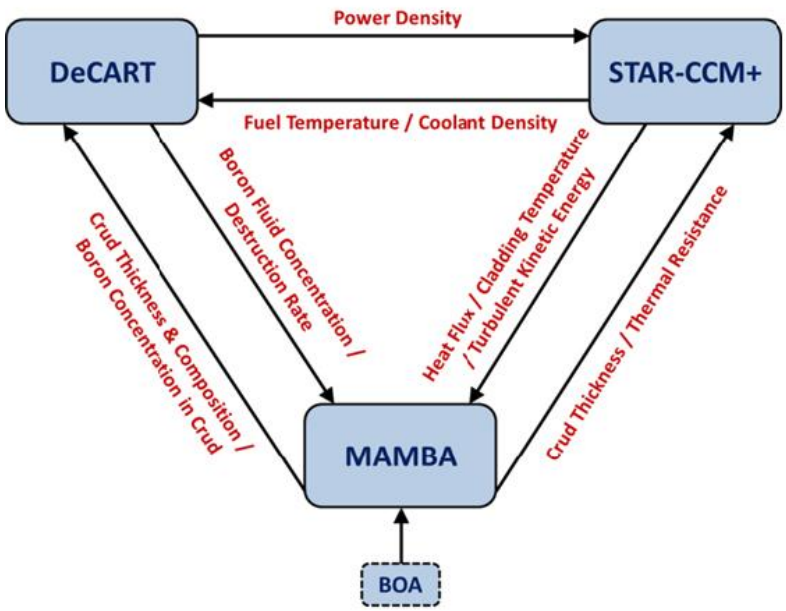

Figure 1.1: Data exchange scheme among DeCART, MAMBA and STAR-CCM+ [6]

1.1 Monte Carlo Method

The Monte Carlo method is very different from deterministic methods [7]. Deterministic transport methods solve the transport equation for the average particle behavior, while Monte Carlo method simulates individual particles to obtain solution. The basic principle is explained as follows [8]: For example, for a single neutron in nuclear reactor, the Monte Carlo method simulates it from its initial emission to its death by absorption or escape from the boundaries of the system. The interactions that occur during the neutron's life can have various frequency and outcomes, and they are randomly sampled and calculated by the interaction laws, which are derived from nuclear particle physics. From this procedure, we can find an obvious drawback of the Monte Carlo method, that the computational cost is very high, especially if the number of simulated particles is high. A large number of particles are required to achieve high accuracy by Monte Carlo

method. This usually limits the application of Monte Carlo method, which is usually reserved for complicated criticality or shielding problems.

Deterministic methods are currently the dominant approach for calculation of neutron transport equations. They used to be the only practical way for full-cores problems, especially when coupling of core neutronics and thermal–hydraulics was necessary.

Monte Carlo codes have a great advantage over traditional deterministic lattice transport codes in that they are capable of detailed and accurate geometry representation than other lattice physics calculations [8]. In addition, theory of homogenization is the standard approach to solving coupled large-scale reactor physics and dynamics problems [9], which is not required for Monte Carlo.

Another advantage of Monte Carlo methods is the simulation of heterogeneous cores, which are very common in the design of next generation nuclear reactors [10]. Compared with deterministic code, Monte Carlo methods do not need space and energy approximations to solve the transport equations, instead, they simulate the behavior of individual particles. Some of the heterogeneous cores are expected to burn Minor Actinides (MA). MA would bear fuels in the fast spectrum, and then a continuous energy representation is even more important to calculate the neutron flux and the reaction rate, instead of a multi-group approach which is common for the thermal reactor cores simulation. Therefore, a continuous-energy Monte Carlo method would be a practical way to model reactor systems with complex geometries and heterogeneous materials.

CHAPTER 2. LITERATURE SURVEY

The improvements of computational power have made it possible to use computationally intensive methods like Monte Carlo for large scale problems and realistic reactor geometries. By looking at the number of recent scientific publications related to nuclear multi-physics applications, it is easy to see that the coupling of Monte Carlo neutronics to CFD and thermal-hydraulics codes is becoming an important research topic.

Researchers have applied coupling between Monte Carlo method and thermal-hydraulic codes in the simulation of innovative fast reactors [10]. In the analysis of Sodium Fast Reactor (SFR) at both fuel assembly and full core scale, the authors coupled Monte Carlo code MCNPX and the sub-channel code COBRA-IV. Figure 2.1 shows the coupled procedure. A significant part of this research is how to deal with the cross-section dependence on the temperature. They handled the temperature dependence of nuclear data with the pseudo material approach, based on JEFF 3.1 data libraries compiled with NJOY at discrete temperature levels.

Neutronics Monte Carlo code MCNPX was also coupled to thermal-hydraulic CFD code CFX, for the cooling channel in the fuel element of FRM II [11]. A FORTRAN extension was developed for CFX that takes the data from a MCNPX mesh tally and converts it into an internal energy source. The temperature of this coupling system converged in two steps. However, the coupling provided very limited new details and no comparison was shown to prove that coupling of MCNPX and CFX improved the simulation of the cooling channel.

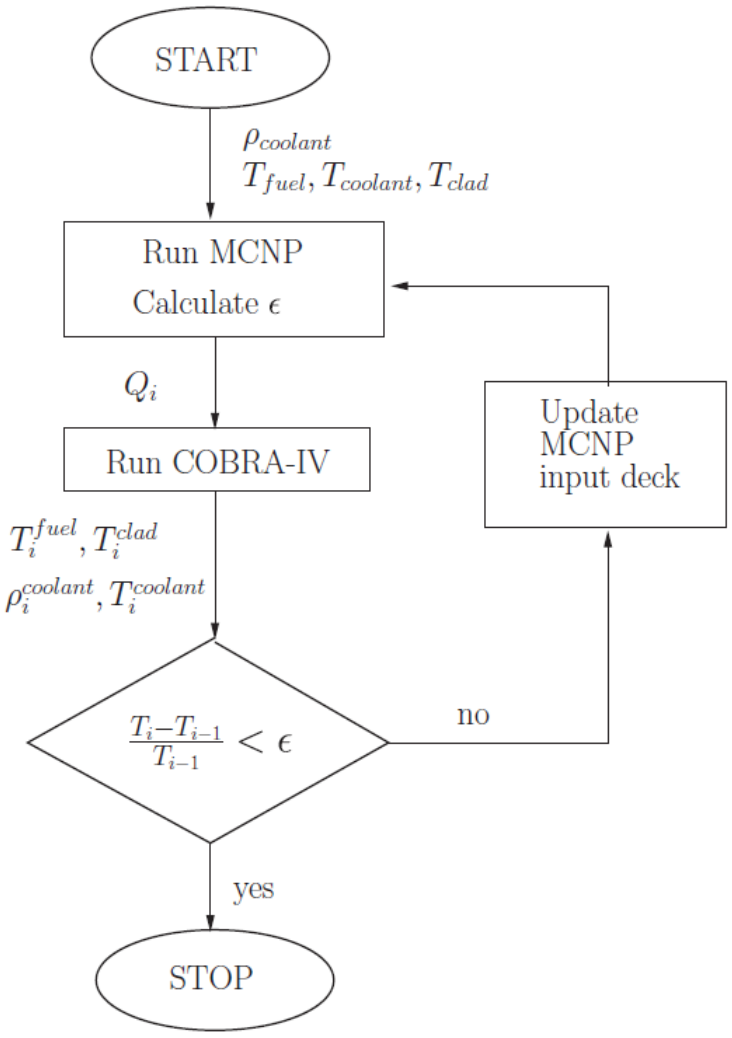

Figure 2.1: Coupling between MCNPX and COBRA-IV for SFR [10]

By utilizing the whole-core neutron transport solutions for neutronics and CFD solution for thermal-hydraulics, high-fidelity has been achieved in modeling of nuclear reactor [12]. The authors utilized Monte Carlo method to validate the coupled deterministic neutron transport and CFD solutions. Compared with previous work, in which Monte Carlo calculations were performed with only limited thermal feedback [13], this is a desirable improvement because CFD has more sophisticated temperature fluid solution.

The Monte Carlo code used is MCNP5 and the CFD code is STAR-CD. NJOY code is used to generate cross-section data from the CFD solution. Figure 2.2 shows the coupling scheme. The analyzed model is a three dimensional 3 by 3 array of PWR fuel pins. The result showed a good agreement in the multiplication factor and the power profile compared to coupling of DeCART and STAR-CD.

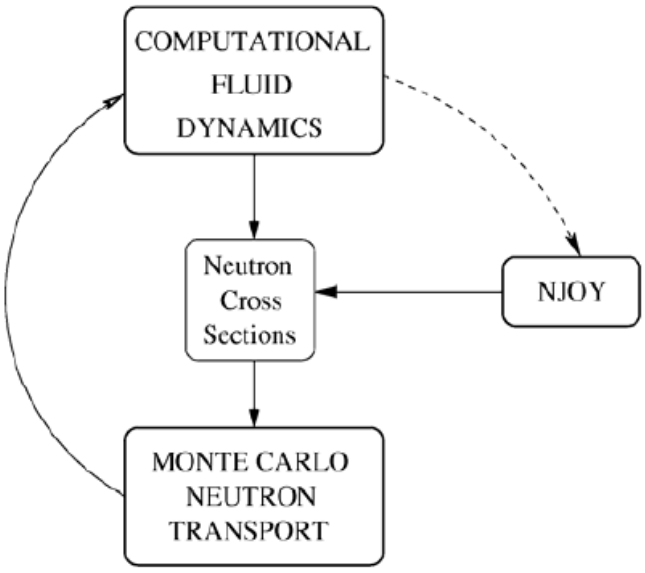

Figure 2.2: Coupling of MC with CFD, neutron cross section generated by NJOY [12]

Progress was also achieved in the depletion analysis by Monte Carlo codes. Researchers at Ben-Gurion University developed BGCore reactor analysis system [14], in which the Monte Carlo transport code MCNP was coupled to a burnup and decay module SARAF developed by the authors. This BGCore can significantly reduce the simulation time while maintaining the accuracy of the results because it used a multi-group (MG) approach for generation of one group depletion cross-sections. The BGCore system is coupled to module THERMO which calculate the temperature distribution in reactor core

by the scheme shown in figure 2.3. The coupling can perform full-core level simulation, with assembly-level resolution.

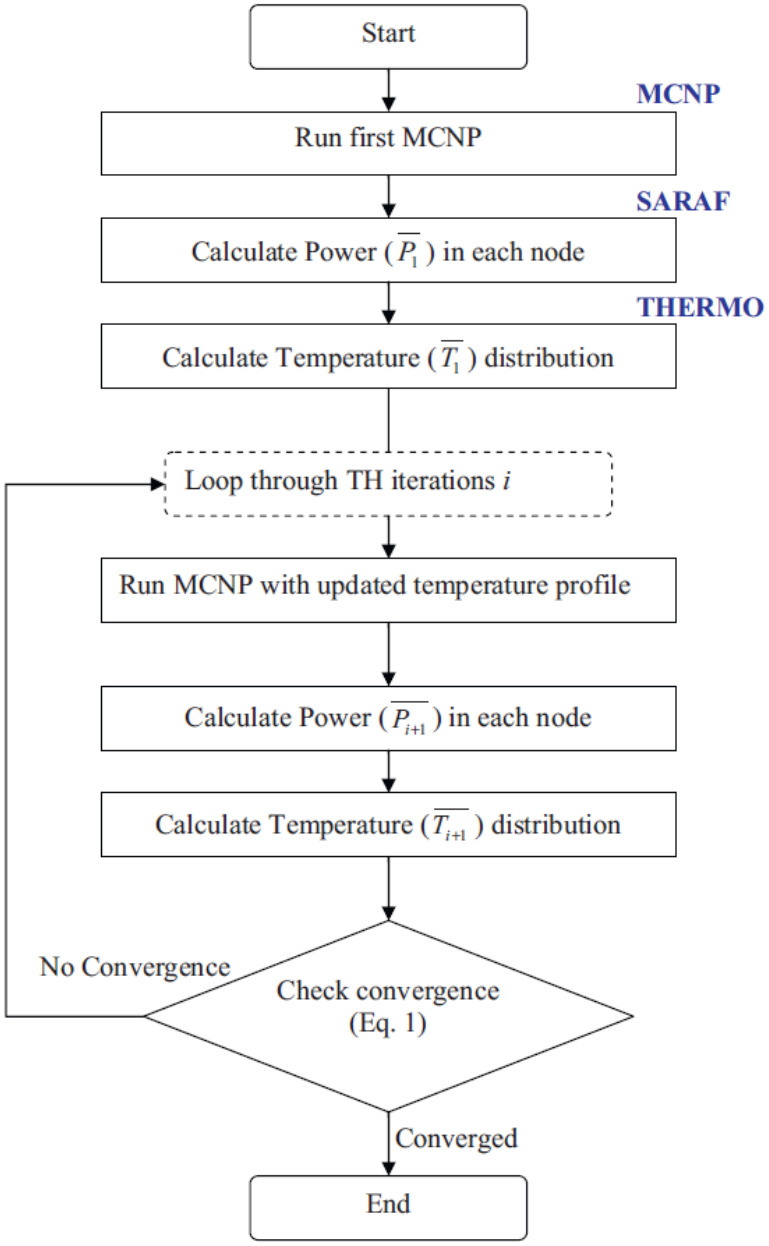

Figure 2.3: Coupling of MC with burnup and decay module SARAF [14]

The coupling results were verified by a code-to-code comparison with a well validated code, DYN3D, and a very good agreement was found both in neutronics and thermal-hydraulics parameters.

In general, most of the coupling systems developed around the world between Monte Carlo and thermal-hydraulics codes share some common features. Researchers used different convergence criteria, but the coupling converges fast, usually in several steps. The results such as temperature and power distribution show good agreement with other codes used for verification purpose. The most obvious drawback is that the computational time is still a limiting factor.

In this thesis a three-dimensional continuous-energy Monte Carlo reactor physics code, Serpent [15], will be coupled with a thermal-hydraulics code RELAP5 [16]. The coupling results will be compared with a deterministic code DeCART [17]. DeCART has an internal thermal-hydraulics feedback solution.

CHAPTER 3. OVERVIEW OF THE CODES

This chapter shows a brief overview of the codes used in the thesis. The code versions of them are Serpent 1.1.18, RELAP5-3D v2.4 and DeCART v2.05.

3.1 Serpent code

Serpent is a three-dimensional continuous-energy Monte Carlo reactor physics burnup calculation code [18], developed at VTT Technical Research Centre of Finland since 2004. Serpent has the capability to build any two or three dimensional configuration, at fuel, assembly or core level. The code is intended specifically for diffusion code multi-group constants generations and other reactor physics calculations.

The Serpent code simulates neutron transport in the geometry based on a combination of conventional surface-to-surface ray-tracing and the Woodcock delta-tracking method [19]. Woodcock delta-tracking method differs quite significantly from the ray-tracing methods used by most of the other neutronics codes. The advantages of the delta-tracking method include reduced computing time and relatively simple handling of complex geometrical objects. Another important method Serpent adopted to substantially reduce the computational time is by “using the same unionized energy grid for all point-wise reaction cross sections” [20]. This method could reduce the grid iteration to a minimum while keep the accuracy.

The suggested applications of Serpent include:

- Generation of homogenized multi-group constants for deterministic reactor simulator calculations;
- Fuel cycle studies involving detailed assembly-level burnup calculations;
- Validation of deterministic lattice transport codes;
- Full-core reactor physics and burnup calculations for research reactors;
- Educational purposes and demonstration of reactor physics phenomena.

3.2 RELAP5-3D code

RELAP5-3D (Reactor Excursion and Leak Analysis Program) is the latest in the RELAP5 code series, developed at the Idaho National Laboratory (INL) [16]. The code is intended for the best-estimate analysis of operational transients and postulated accidents in water-cooled nuclear power plants and related systems. Additional capabilities include space reactor simulations, gas cooled reactor applications, fast breeder reactor modeling, and cardiovascular blood flow simulations.

The RELAP5-3D hydrodynamic model is a transient, two-fluid model for flow of a two-phase vapor/gas-liquid mixture. The model solves eight field equations for eight primary dependent variables. These primary dependent variables are pressure (P), phasic specific internal energies (U_g , U_f), vapor/gas volume fraction (void fraction) (α_g), phasic velocities (v_g , v_f), non-condensable quality (X_n), and boron density (ρ_b).

The non-homogeneous and non-equilibrium model for the two-phase system is solved by a fast, partially implicit numerical scheme to permit economical calculation of system

transients. Some approximations are included in the hydrodynamic model for invoking simpler hydrodynamic models. For example, the homogeneous flow, thermal equilibrium, and frictionless flow models. These options can be used independently or in combination.

3.3 DeCART code

DeCART (Deterministic Core Analysis based on Ray Tracing) is a three-dimensional whole-core neutron transport code capable of core simulation of Pressurized Water Reactor (PWR) and Boiling Water Reactor (BWR) [21]. Unlike conventional reactor physics simulation codes, DeCART does not need a priori homogenization or group condensation. The code can solve steady-state eigenvalue problem, as well as transient fixed source problem. Method of Characteristic (MOC) is used to deal with the heterogeneity at the pin cell level [17]. DeCART obtains multi-group cross-section data from a cross-section library normally used in lattice transport codes.

DeCART incorporates both the neutronic and thermal-hydraulics solution modules, as well as an iterative solution logic controlling the alternate execution of the two modules and the subsequent cross section update. DeCART takes into account both the Doppler and coolant number density effects in order to incorporate the thermal feedback effect the flux calculation. DeCART defines uniform cross section regions (UXR) within each pin cell. The details on how DeCART calculates fuel temperature distribution and coolant temperature and density could be found in [17].

CHAPTER 4. BENCHMARK PROBLEM

Even though there is no limitation imposed by the code on the size of the computational domain (other than computational time and computer memory), for the computational efficiency it is preferable to use a problem as small as practically possible, while still maintaining all desirable solution features. Therefore, for the purposes of coupling development and its verification, a single assembly problem was used. All the features and capabilities of the coupling can be demonstrated based on the selected single assembly problem.

4.1 Single assembly description

The assemblies analyzed in this thesis for code coupling are based on OECD/NEA and U.S. NRC PWR MOX/UO2 core transient benchmark [1]. This benchmark is a well-defined problem that provides the framework to assess the ability of modern reactor kinetic codes to predict the steady-state and transient response of a core partially loaded with weapons grade MOX fuel. This benchmark employs many of the characteristics of the NEACRP L-335 PWR benchmark proposed by Finnemann in 1991 [22], but it was specified without the need for spatial homogenization.

The assemblies used in this benchmark are based on 17x17 Westinghouse design. Both UO2 and MOX assemblies are adopted with some modifications based on the original benchmark. Each assembly has 264 fuel pins and 25 guide tubes. Moreover, MOX fuel rods have three different types. The assemblies configuration simulated are shown in Figures 4.1 and 4.2.

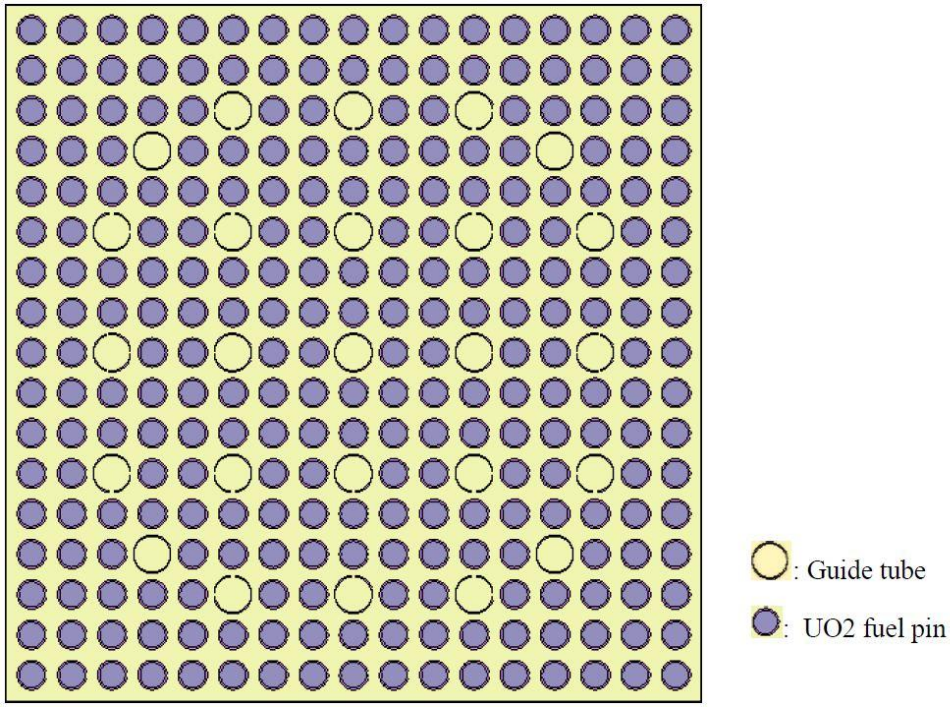

Figure 4.1: UO2 4.2% Fuel Assembly

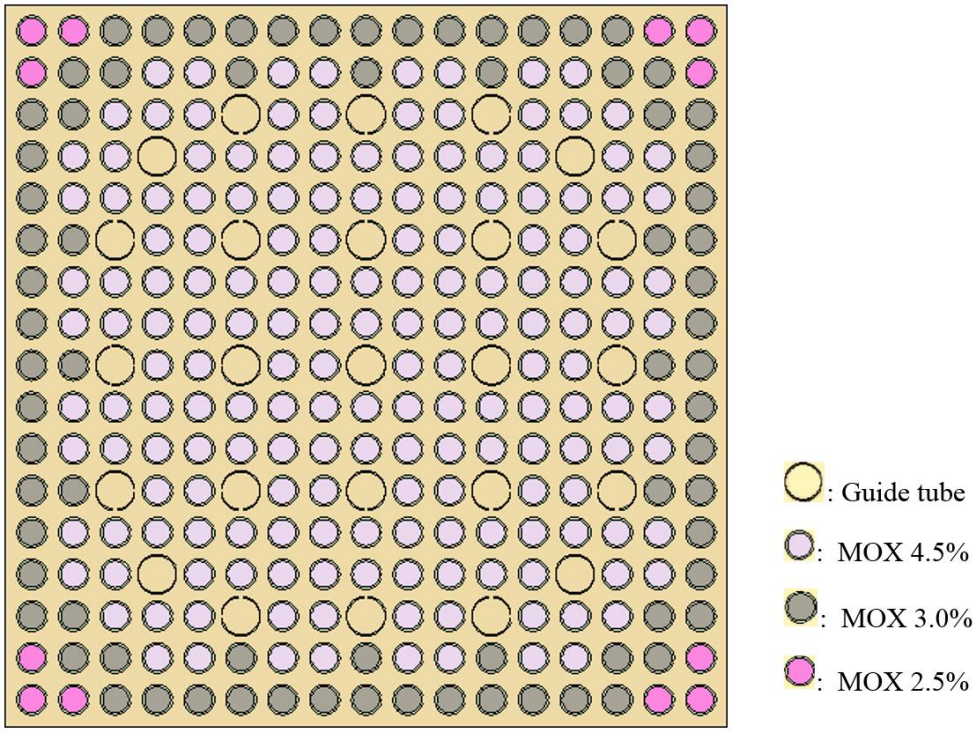

Figure 4.2: MOX 4.0 % Fuel Assembly

4.2 Assembly dimensions and material composition

Table 4.1 shows the material composition used in the assemblies. UO2 material is based on the 4.2% UO2 assembly from the benchmark, while MOX material is based on the 4.0% MOX assembly. Gap in the fuel rod is not considered. The same type of Zircaloy-2 material is used as cladding for fuel pin and guide tube.

Table 4.1: Material composition

<table>
<tr><th>Material type</th><th>Density (g/cm^3)</th><th colspan="2">Composition</th></tr>
<tr><td>UO_2 4.2%</td><td>10.24</td><td colspan="2">U-235: 4.2 wt%, U-238: 95.8 wt%</td></tr>
<tr><td rowspan="3">MOX 4.0%</td><td rowspan="3">10.41</td><td>Corner zone:
2.5 wt% Pu-fissile</td><td rowspan="3">Uranium vector:
234/235/236/238 =
0.002/0.2/0.001/99.797 wt%

Plutonium vector:
239/240/241/242 =
93.6/5.9/0.4/0.1 wt%</td></tr>
<tr><td>Peripheral zone:
3.0 wt% Pu-fissile</td></tr>
<tr><td>Central zone:
4.5 wt% Pu-fissile</td></tr>
<tr><td>Clad</td><td>6.504</td><td colspan="2">Zircaloy-2: Zr/Sn/Fe/Cr/N = 98.23/1.50/0.12/0.10/0.05 at%</td></tr>
<tr><td>Coolant</td><td>0.75206</td><td colspan="2">Water at 560K and 15.5 MPa</td></tr>
</table>

Table 4.2 shows the assembly dimensions. 30 cm of coolant is added at the top and bottom of the single assemblies as reflector.

Table 4.2: Assembly dimensions

Properties	value	unit
Active fuel length	365.76	cm
Assembly pitch	21.42	cm
Pin pitch	1.26	cm
Hydraulic Diameter	1.1979	cm
Heated diameter	1.3472	cm

Table 4.3 and 4.4 below give the dimensions of fuel pins and guide tubes. As indicated above, gap is not considered in the coupling simulation, so both the UO2 and MOX fuel are surrounded only by clad material.

Table 4.3: Fuel pin dimensions

Material	Outer radius	Unit
Fuel	0.3951	cm
Clad	0.4583	cm

Table 4.4: Guide tube dimensions

Material	Outer radius	Unit
Water	0.5624	cm
Clad	0.6032	cm

Table 4.5 gives the boundary conditions used in the simulation. The inlet flow rate and assembly power was obtained by dividing the total core flow rate and total core power by the number of assemblies.

Table 4.5: Boundary conditions

Name	Value	Unit
Inlet temperature	560.00	K
Inlet flow rate	82.12	kg/s
Outlet pressure	15.50	MPa
Single assembly power	18.47	MW

4.3 Thermal-physical properties

The following fuel and cladding thermal-physical properties are used in this thesis, based on the NEACRP 3-D LWR Core Transient Benchmark [22]. For simplification, both UO2 and MOX use the same thermal-physical properties. Equation 4.1 and 4.2 are the thermal conductivity of fuel and clad, respectively. Equation 4.3 and 4.4 are the heat capacity of fuel and clad, respectively. Finally, Equation 4.5 and 4.6 are the density of fuel and clad, respectively.

$$k_{fuel} = 1.05 + 2150 \cdot (T - 73.15)^{-1} \quad W/(m \cdot K) \tag{4.1}$$

$$k_{clad} = 7.51 + 2.09 \times 10^{-2} T - 1.45 \times 10^{-5} T^2 + 7.67 \times 10^{-9} T^3 \quad W/(m \cdot K) \tag{4.2}$$

$$c_{p,fuel} = 162.3 + 0.3038 \cdot T - 2.391 \times 10^{-4} \cdot T^2 + 6.404 \times 10^{-8} \cdot T^3 \quad J/(kg \cdot K) \tag{4.3}$$

$$c_{p,clad} = 252.54 + 0.11474 \cdot T \quad J/(kg \cdot K) \tag{4.4}$$

$$\rho_{fuel} = 10240 \quad kg/m^3 \tag{4.5}$$

$$\rho_{clad} = 6504 \quad kg/m^3 \tag{4.6}$$

CHAPTER 5. COUPLING SCHEME

In this chapter, the coupling scheme for Serpent and RELAP5-3D and the cross-section treatment method is introduced. Also, Serpent and DeCART models are verified to be consistent and the convergence criteria are determined for the coupling.

5.1 Coupling scheme

The coupling of Serpent and RELAP5-3D is based on explicit coupling: the two codes are executed serially and exchange information at every coupling step. Axially, the assemblies are divided into 24 equidistant nodes. Changes in coolant temperature and density, and Doppler broadening of absorption are the three main temperature feedbacks. Therefore, data exchange between Serpent and RELAP5-3D involves material temperatures, coolant densities and fuel axial power distribution. The coupling procedure is summarized in the following steps and Figure 5.1 illustrates how the data are exchanged between Monte Carlo code Serpent and RELAP5-3D.

1) RELAP5-3D is executed with a uniform heat source in the axial direction. After completion, temperatures of fuel, coolant and cladding, and coolant densities are extracted from the output for all the 24 axial nodes.

2) The temperatures of fuel, coolant and cladding, and coolant densities are used for material definition in corresponding axial node in the Serpent model.

3) The newly generated Serpent input is executed. After completion, axial power is

extracted from the output for all the 24 axial nodes.

4) The axial power is used for the heat source definition in the corresponding axial node in the RELAP5-3D model. The newly generated RELAP5-3D input is executed. New results of temperatures of fuel, coolant and cladding, and coolant densities are obtained.

5) The steps 2-4 are repeated until convergence. The axial power distributions from the last two coupling iterations are compared according to the convergence criteria. If the convergence criteria are not met, steps 2-4 are repeated.

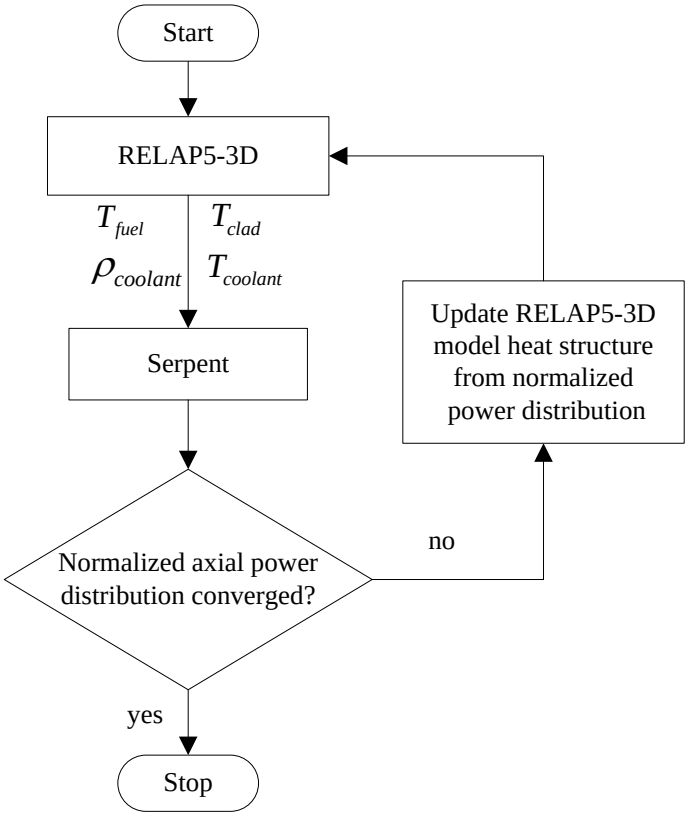

Figure 5.1: Coupling scheme between Serpent and RELAP5-3D

The DeCART code has an option to run with or without thermal-hydraulics feedback. The geometry of the DeCART model is also divided into 24 equidistant axial nodes. If DeCART is executed without thermal-hydraulics feedback, consistent comparison of axial power distribution can be made between Serpent and DeCART to verify Serpent model. Furthermore, if DeCART runs with internal thermal-hydraulics feedback, its result can be compared with Serpent/RELAP5-3D, to verify the coupling.

5.2 Cross-section handling

Temperature dependence of the microscopic cross section is an important part of the thermal feedback effect. Three methods are summarized in previous work [10] and [12].

1) The first method is based on pre-generated, Doppler-broadened cross-sections library, prepared beforehand using codes like NJOY (a cross-section processing code, [23]). An explicit library is generated for every nuclide, with a small temperature increment (usually 2-5 K) between the lowest and highest temperature expected during the simulation. The Monte Carlo method uses cross section at temperature that is nearest to the local calculated temperatures. This is a very practical approach, however, inherent error is introduced by the increment of the temperature interval.

2) The second method is similar to the first one, but the library is generated with a larger temperature increment (about 25-50 K).In order to obtain cross-section at the local calculated temperature, an interpolation method is used based on the interval the temperature falls in. This approach has the potential to be more

precise than the first method, and has been shown to generate more accurate results for some cases [10].

3) The most accurate method is the On-The-Fly (OTF) Doppler Broadening [24]. The implementation of OTF Doppler broadening in Monte Carlo involves high precision fitting of Doppler broadened cross-sections over a wide temperature range, with parameters that depend on the energy and temperature. Comparing with the previous two methods, this method is more straightforward for the end-user and "allow the Monte Carlo simulation account for a continuous distribution of temperature ranges throughout the problem geometry" [24].

Serpent uses continuous-energy ACE format data library generated using NJOY-99.259 with 0.01 fractional reconstruction tolerance. For Doppler broadening, Serpent uses "interpolation method for producing effective intermediate temperature cross sections from two libraries generated at different temperatures" [8]. The atomic fraction of the low temperature isotope is calculated from:

$$f_{low}(T) = \frac{\sqrt{T_2} - \sqrt{T}}{\sqrt{T_2} - \sqrt{T_1}} \tag{5.1}$$

Where T is the interpolation temperature. T_1 and T_2 are the low and high temperatures of the cross section libraries. Consequently, the fraction of the high temperature isotopes is $f_{high}(T) = 1 - f_{low}(T)$.

5.3 Consistency study of Serpent and DeCART models

The verification of Serpent/RELAP5-3D coupling is based on the comparison with DeCART results, specifically the multiplication factor and the axial power distribution. Consistency of DeCART and Serpent models is shown through a series of problems of increasing difficulty:

1) There are discrepancies resulting from the difference in cross-section libraries used by Serpent and DeCART. DeCART uses a library based on a combination of ENDFB/VI and ENDFB/VII [25]. Serpent 1.1.18 has five cross-section libraries, the latest three libraries will be adopted (JEFF-3.1.1, ENDFB/VI.8 and ENDFB/VII) in this work. Serpent cross-section library study will be performed to find the library which is the most consistent with DeCART.

2) After choosing the most appropriate neutron library, criticality of 2-dimensional single-assembly model will be compared at cold and hot conditions, in order to estimate the consistency of the thermal feedback in the cross-section library.

3) Finally, 3-dimensional models are developed from the consistent 2-dimensional models. Multiplication factor and axial power distribution are compared to demonstrate the consistency of DeCART and Serpent 3-D models.

5.3.1 Consistency of 2-D models

The purpose of this section is to find the Serpent cross-section library which is most consistent with DeCART. The multiplication factor of 2D assemblies is compared under

operating conditions (described in section 4.2) with no thermal-hydraulics feedback. Temperature of fuels, cladding and moderator are the same in Serpent and DeCART.

Table 5.1: Library study of 2-D models, fixed feedback hot conditions

Multiplication Factor				
Assembly	DeCART	Serpent		
		ENDFB/VII	ENDFB/VI.8	JEFF-3.1.1
UO2	1.41860	1.42810	1.42334	1.42726
MOX	1.33530	1.34521	1.34076	1.34351

(Note that every eigenvalue in Table 5.1 by Serpent has a statistical error of 1.3E-05. This is also valid for Table 5.2).

The Serpent cross-section library ENDFB/VI.8 yields the closest multiplication factor to DeCART. Therefore, this library will be used for all following simulations.

Table 5.2: Difference in the libraries for 2-D models, fixed feedback

Multiplication Factor (Serpent library: ENDFB/VI.8)			
Assembly	DeCART	Serpent	Difference (pcm)
UO2, cold	1.44462	1.44932	470
UO2, hot	1.41860	1.42334	474
MOX, cold	1.37888	1.38356	468
MOX, hot	1.33530	1.34076	546

From the results presented in Table 5.2, it is obvious that the cross-section libraries used by Serpent and DeCART have some differences. This difference is inherent to the cross-section library and exists at all thermal-hydraulics conditions, but we expect this difference to be constant, provided all other model parameters are the same. To show this, we run the same model with a fixed fuel and moderator temperature of 300K, known as a cold state.

The difference between DeCART and Serpent is about 500 pcm, and is constant for UO2 fuel at different thermal-hydraulics conditions (hot vs. cold). However, it appears that fuel temperature feedback is stronger in DeCART by about 80 pcm. For the purpose of this work, this difference is small, and it can be concluded that Serpent and DeCART thermal-hydraulics feedback are consistent.

5.3.2 Consistency of 3-D models

3-D models for Serpent and DeCART are developed from corresponding 2-D models in section 5.3. Similarly as in the previous section, the 3-D model of Serpent and DeCART was compared with different fuel (UO2 and MOX) and thermal-hydraulics conditions (hot and cold). In 3-D, the difference between DeCART and Serpent is about 1100 pcm for UO2 fuel and 1500 pcm for MOX fuel. The difference between different thermal-hydraulics conditions (hot vs. cold) is constant.

Table 5.3: Difference in the libraries for 3-D models, fixed feedback

Multiplication Factor (library: ENDFB/VI.8)			
Assembly	DeCART	Serpent	Difference (pcm)
UO2, cold	1.43912	1.45007	1095
UO2, hot	1.41325	1.42495	1170
MOX, cold	1.37380	1.38797	1417
MOX, hot	1.33048	1.34658	1610

(Note that every eigenvalue in Table 5.3 by Serpent has a statistical error of 1.5E-05.)

In addition, the normalized axial power comparisons of Serpent and DeCART are shown on Figures 5.2 and 5.3 for cold and hot state, respectively. The normalization is done by dividing neutron flux at every node by the sum of neutron flux at all nodes.

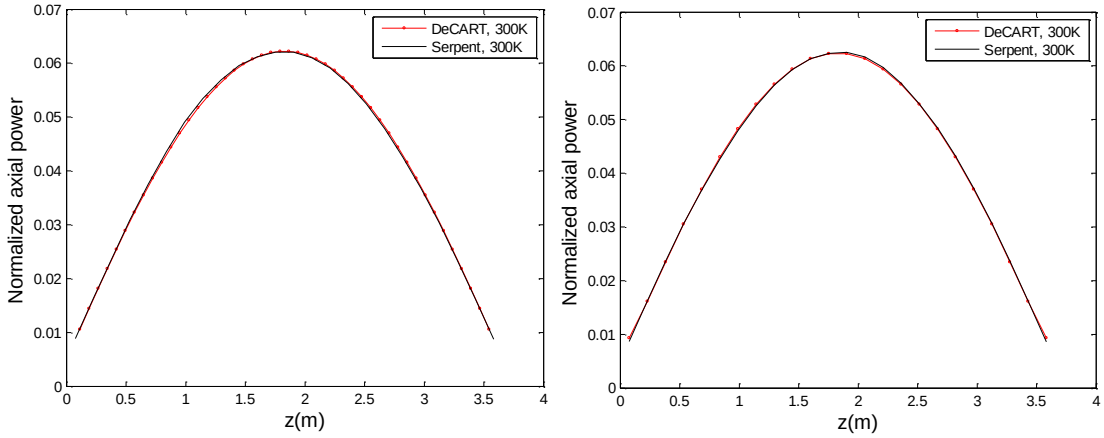

Figure 5.2: Normalized axial power distribution for 3-D UO2 (left) and MOX (right) single assembly comparison between Serpent and DeCART, at cold state

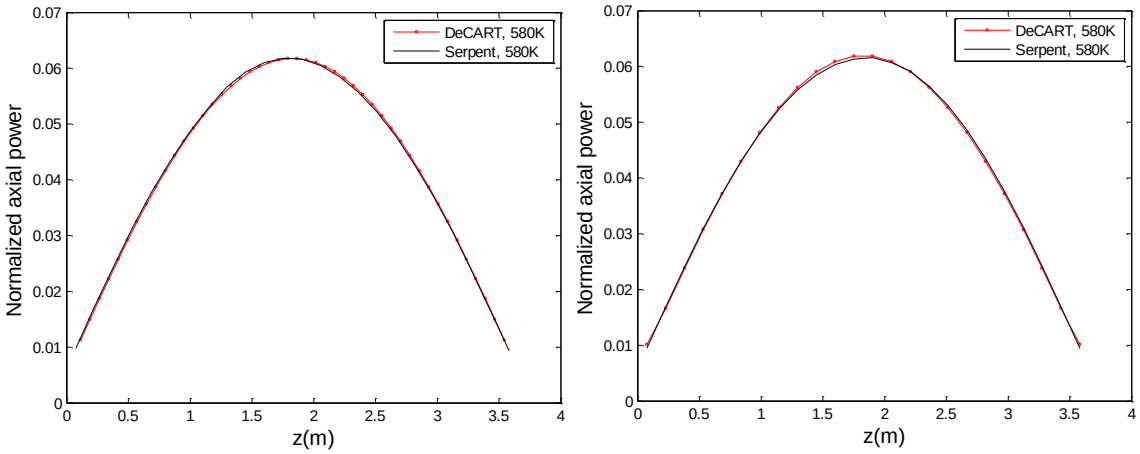

Figure 5.3: Normalized axial power distribution for 3-D UO2 (left) and MOX (right) single assembly comparison between Serpent and DeCART, at hot state

The axial power is in excellent agreement between Serpent and DeCART. This, and the constant differences in criticality, shows that the Serpent and DeCART models are consistent with each other. Based on the above results, we have high confidence that the 3-D DeCART model with thermal-hydraulics feedback can be used as the reference solution for the coupled Serpent/RELAP5 developed in this thesis. If the two methods

yield consistent results in multiplication factor and axial power distribution, we can prove that the coupling of Serpent and RELAP5 works correctly.

5.4 Convergence criteria

Serpent is a Monte Carlo code. As such, insufficient number of source particles, active cycles and inactive cycles used will introduce large statistical error. Inactive cycles are cycles that are used to find initial fission source distribution, before any particles are tracked and reaction rates calculated. A typical lattice calculation requires, as recommended by Serpent manual, at least 20 inactive cycles, 500 active cycles and 5000 source neutrons. In the thesis, all the Serpent models use 100 inactive cycles and 1000 active cycles.

In Monte-Carlo method each solution is statistically the same, but numerically different, which is detrimental to the coupling with deterministic method (e.g. RELAP5). The statistical accuracy can be improved by increasing the number of source neutrons. Therefore, a study is performed to find the number of source neutrons sufficient to reduce statistical variability to a negligible level.

5.4.1 Serpent sensitivity to number of source neutrons

To find appropriate number of source neutrons, 3-D UO2 and MOX single assembly models are calculated by Serpent, with number of 5K, 10K, 20K, 100K, 500K and 1 million source neutrons per cycle. For every number of source neutrons, the calculation is repeated five times. The five normalized axial power distributions are compared to analyze their statistical variability. The purpose is to find a satisfactory number of source

neutrons to use for the coupling. In this work, it was assumed that sufficient statistical accuracy is achieved when the peak axial power varies by less than 1% and peak axial power location varies by less than 5% of node length (7.62 cm).

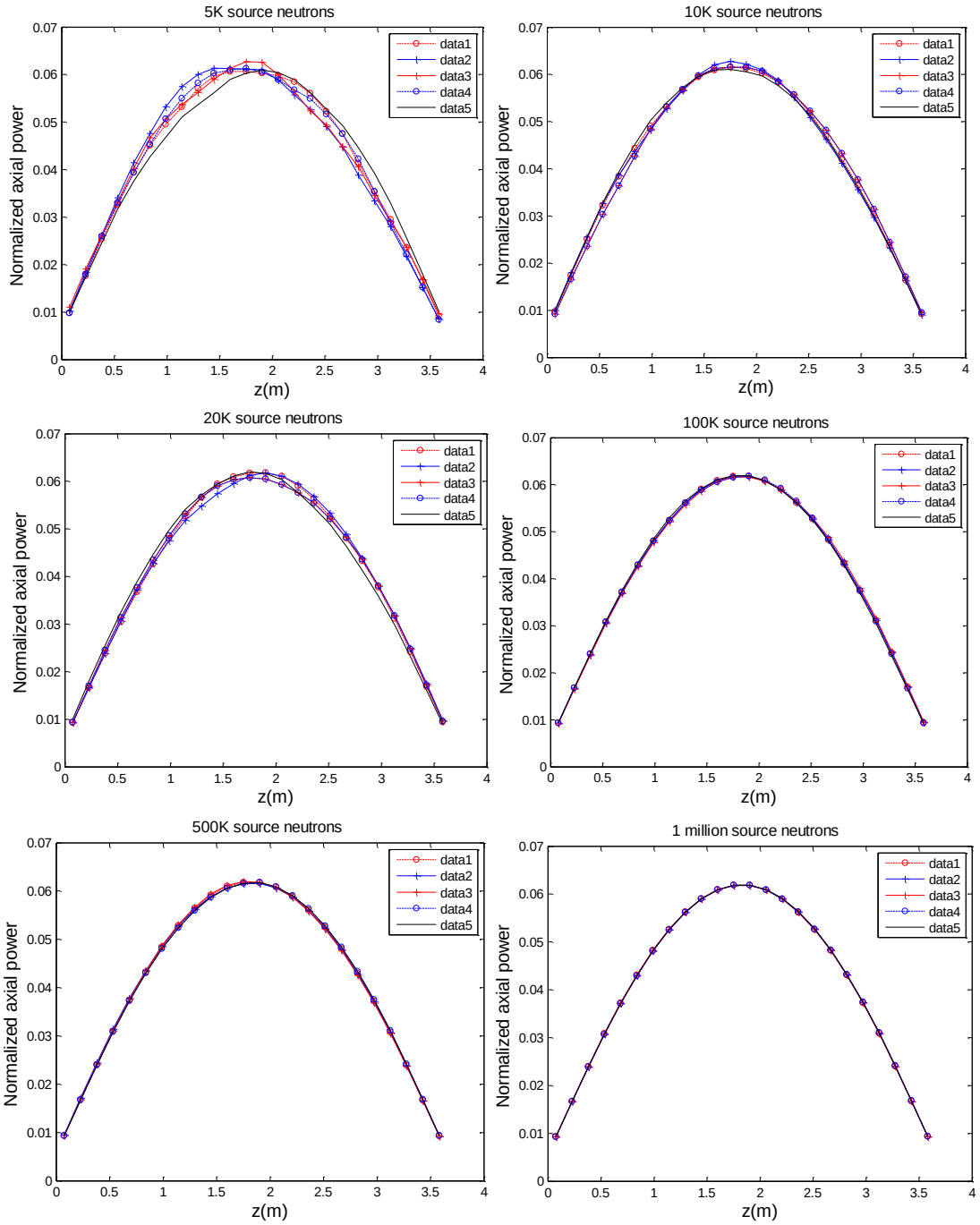

Figure 5.4: Normalized axial power distribution for different number of source particles, UO2 single assembly model

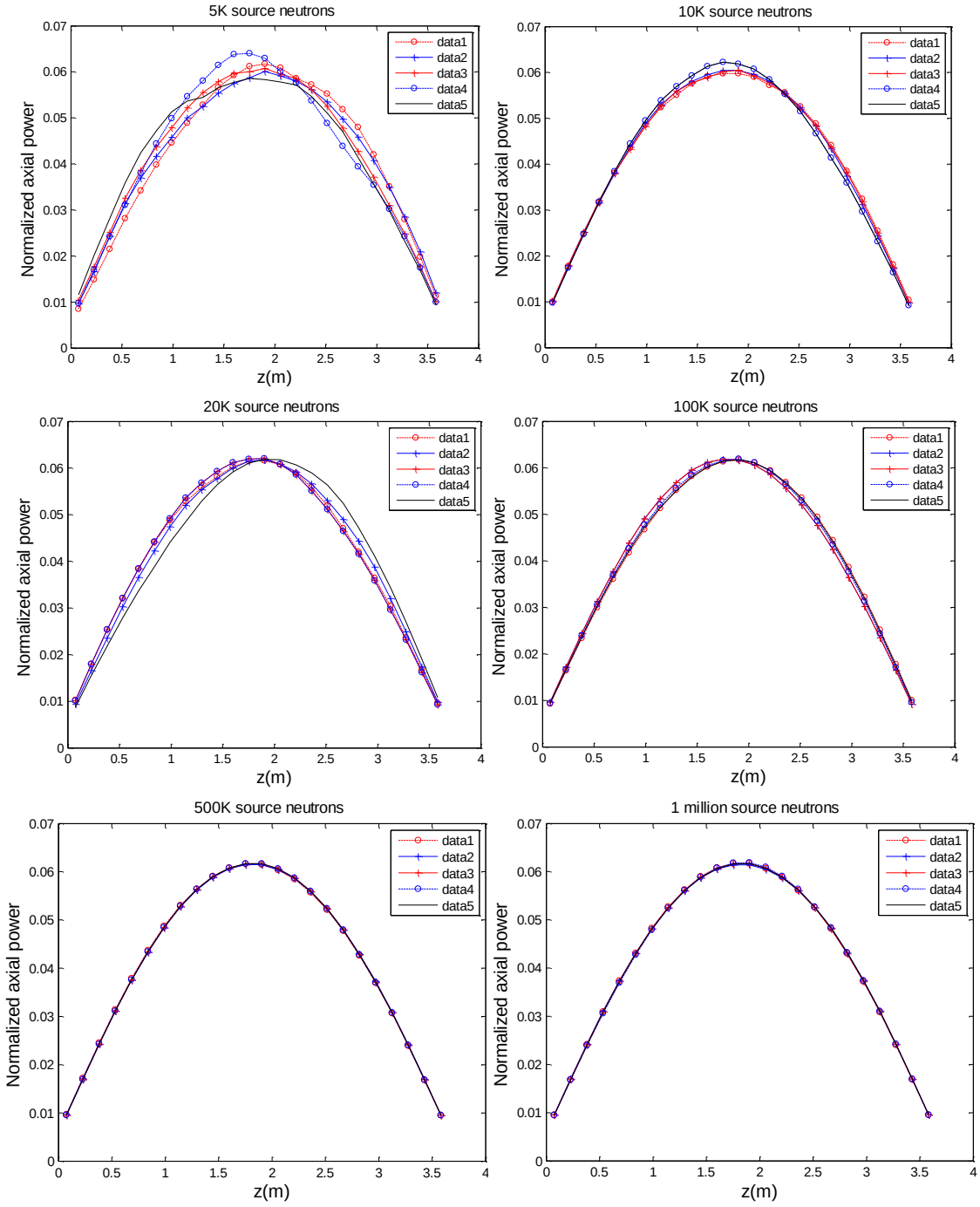

Figure 5.5: Normalized axial power distribution for different number of source particles, MOX single assembly model

As can be seen in Figures 5.4 and 5.5, noticeable difference exists when the number of source particles is too small. More source neutrons give more accurate Monte Carlo

results, but the computational cost is higher. Based on the obtained results, 1 million source neutrons is required to achieve the desired low statistical variability. For both UO2 and MOX assembly models, the peak axial powers for the five cases vary by less than 1%, and peak axial power locations vary by less than 5% of node length. Therefore, Serpent will use 1 million source particles for coupling with RELAP5-3D.

5.4.2 Serpent Statistical Error

Even though 1 million source neutrons, as indicated in section 5.4.1, are sufficient to satisfy our statistical accuracy requirement, there still exists some statistical error in the Monte Carlo solution. The power profile and multiplication factor calculated by Monte Carlo methods have inherent uncertainty. Therefore, rather than pick an arbitrary convergence criterion, the statistical uncertainty of Monte Carlo methods should be considered and used to determine the accuracy of coupled simulation.

Here, the statistical uncertainties for the two different Serpent models will be quantified. Serpent simulations of 3-D models for UO2 and MOX single assemblies are repeated 100 times. The results are shown in Figures 5.6 and 5.7. Every execution of Serpent produces a unique normalized axial power distribution. Each model has 24 axial nodes, and therefore each axial node will have 100 normalized axial power values. These 100 values satisfy the normal distribution. The values are fitted to the normal distribution to obtain standard deviation.

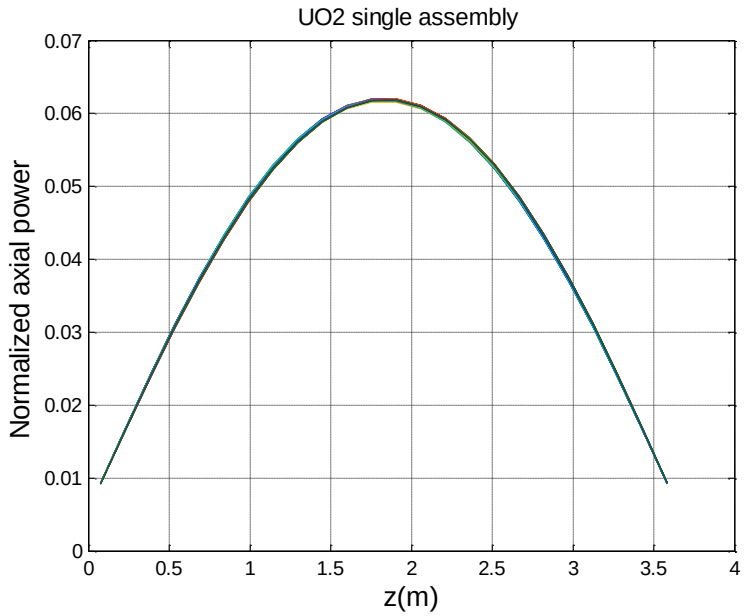

Figure 5.6: Statistical error study of UO2 assembly.

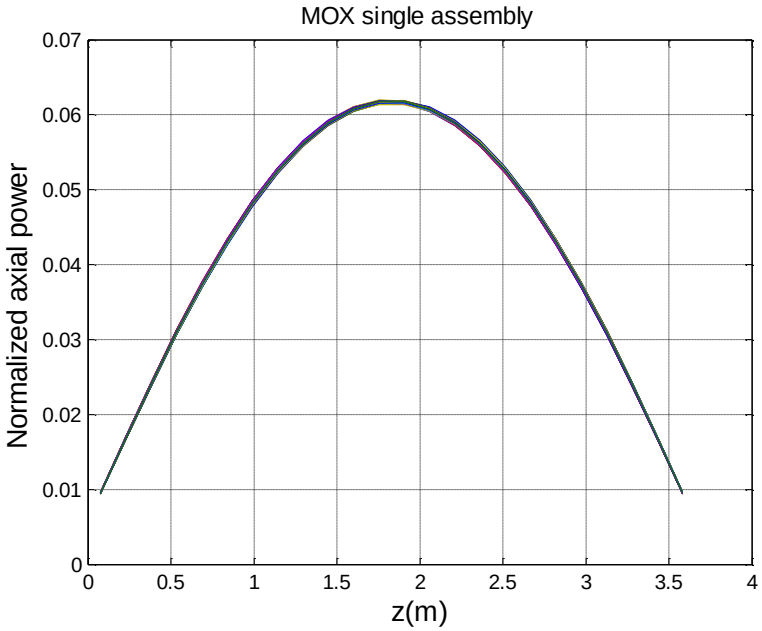

Figure 5.7: Statistical error study of MOX assembly.

The mean and 1 standard deviation of the above results are shown in Figures 5.8 and 5.9.

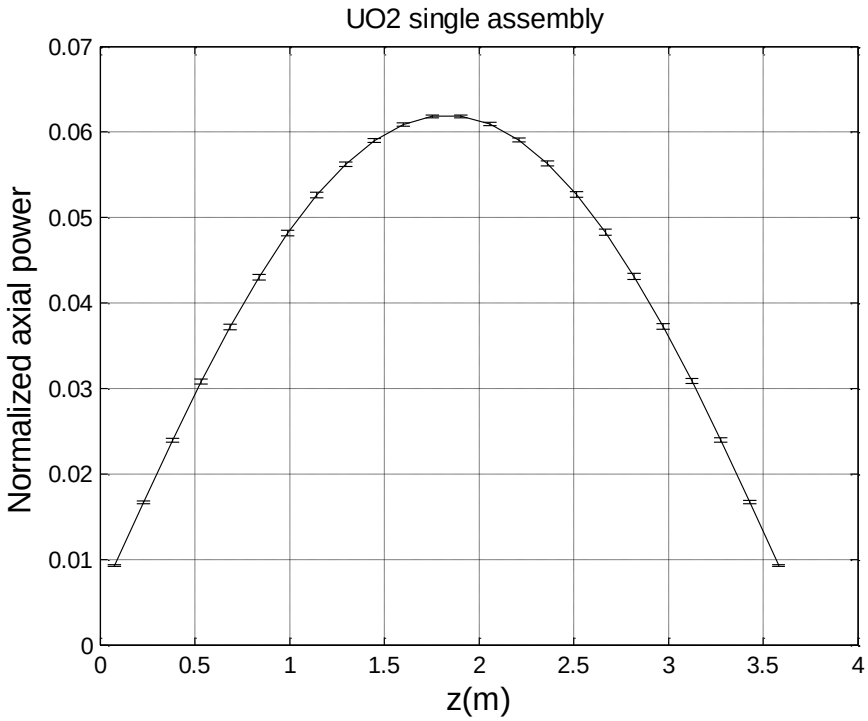

Figure 5.8: Error bar of normalized power distribution, UO2 single assembly

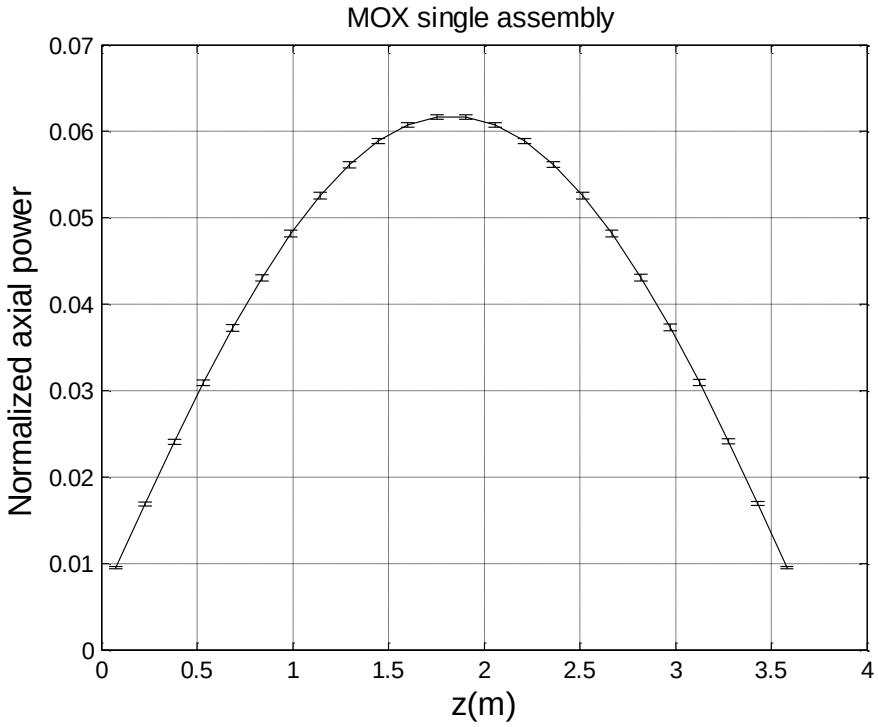

Figure 5.9: Error bar of normalized power distribution, MOX single assembly

The standard deviation can be used to estimate convergence of the coupled Serpent/RELAP5-3D. For every coupling iteration, the normalized axial power distribution is compared with the normalized axial power distribution from the previous coupling iteration. If more than 22 (24*95%=22.8) of the 24 axial power data points fall within 2 standard deviations of the axial power from the previous coupling iteration, the coupling is considered to be converged.

CHAPTER 6. CONVERGENCE AND RESULTS

In this part, coupled Serpent/RELAP5-3D results are compared with results obtained with DeCART. First, converged coupled simulation is achieved. The convergence criteria have been introduced in section 5.4.

6.1 Convergence of the coupling

The coupled Serpent/RELAP5-3D normalized axial power distribution is plotted and compared with that of the previous coupling step. If more than 22 of the 24 points fall within the statistical error of 2 standard deviations of the previous coupling step, the coupling is considered to be converged.

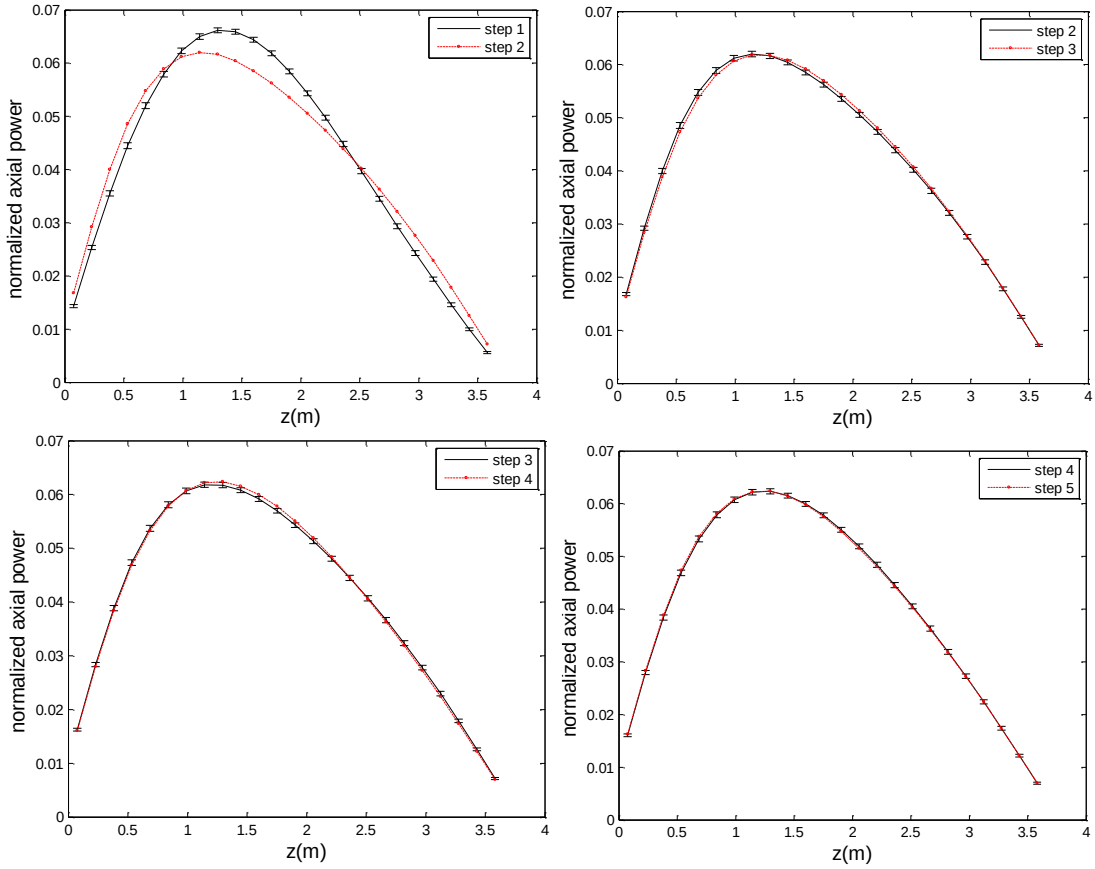

Figure 6.1: Convergence process of coupling for UO2 models.

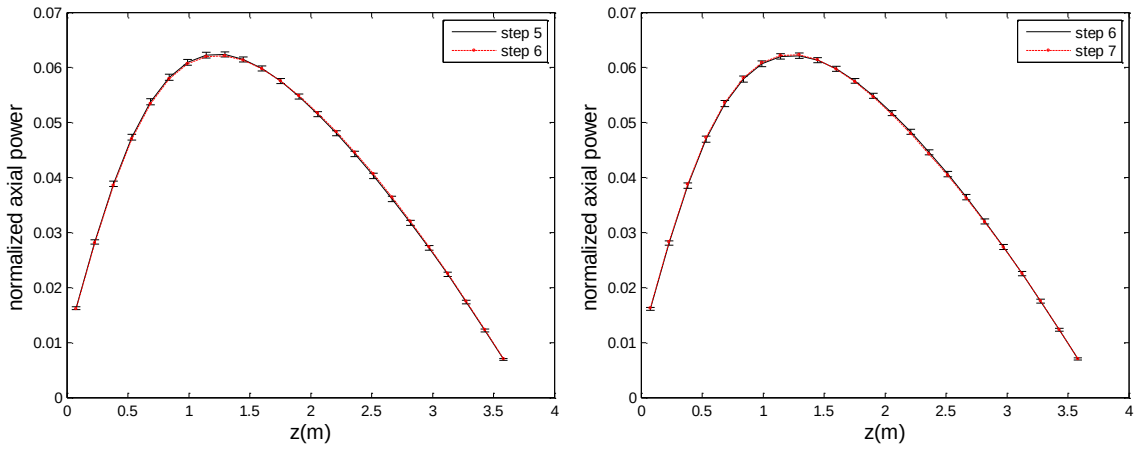

Fig 6.1 (cont.)

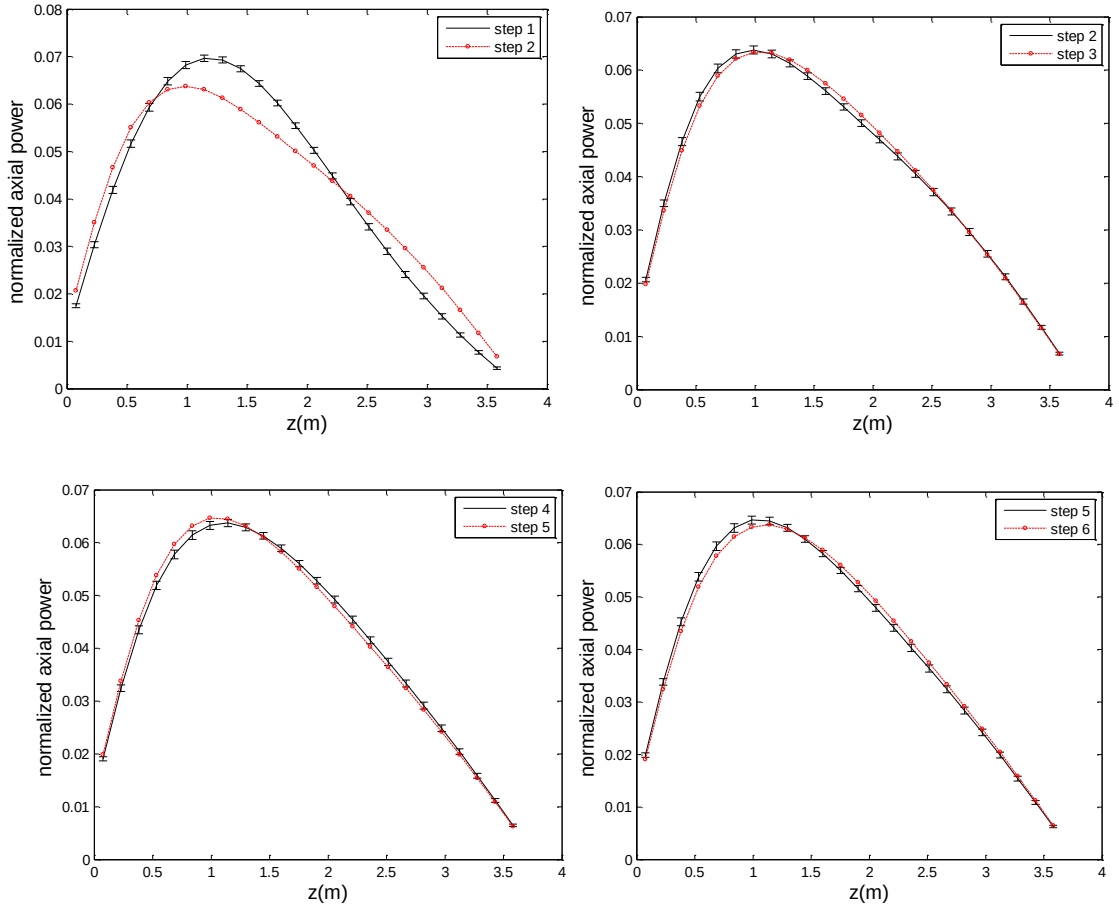

Figure 6.2: Convergence process of coupling for MOX models

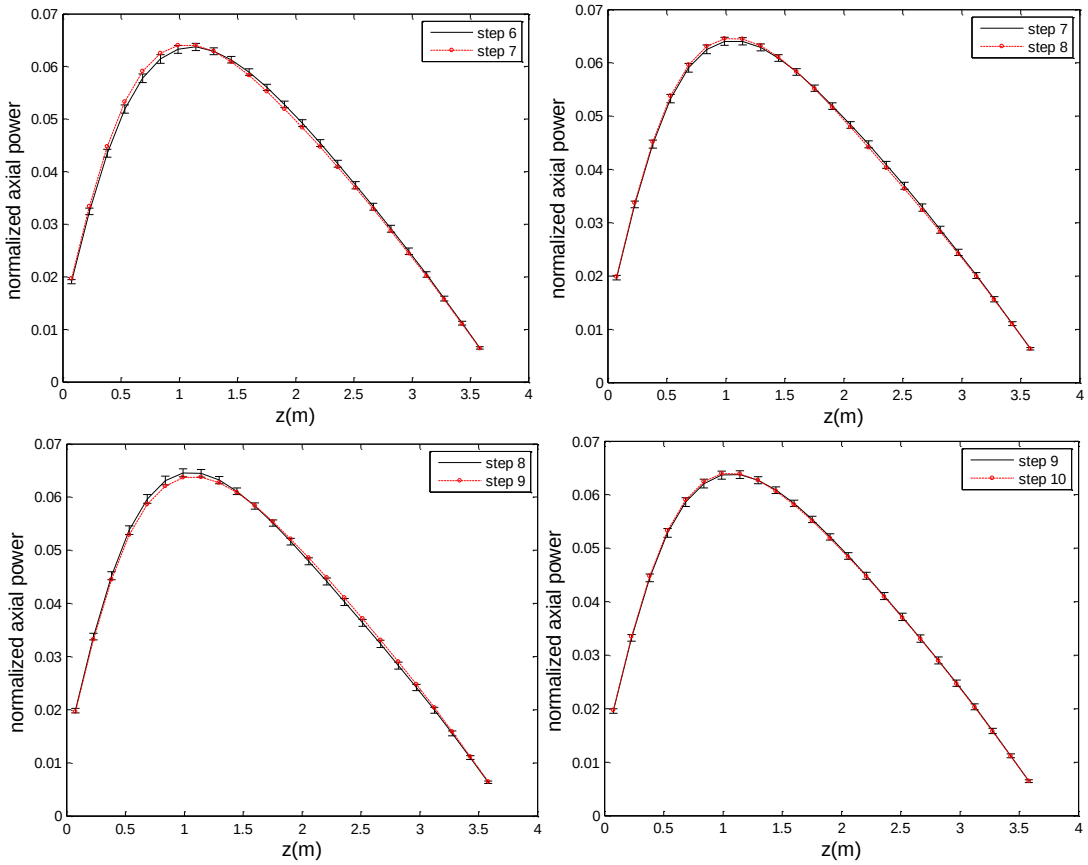

Fig 6.2 (cont.)

Figures 6.1 and 6.2 show that UO2 single assembly model coupling is converged at step 7, while the MOX single assembly model coupling is converged at step 10. Without the thermal-hydraulics feedback, Serpent will calculate a cosine-shaped axial power distribution. When the thermal-hydraulics feedback is introduced, the peak moves towards the bottom because the coolant mass density is higher there, as is shown in Figure 6.3.

The computer cluster used for coupling uses Intel X5650 (6 core) 2.66GHz processors. Each node has 12 cores (2 CPUs) and 96 GB of RAM, and 2 nodes are used for the coupling. Every case is executed with 100 inactive cycles, 1000 active cycles and 1 million source neutrons per cycle.

6.2 Other convergence criteria

The previous and current research shows that Monte Carlo coupling with thermal-hydraulics codes converges very fast, within about 10 coupling steps. However, previous coupling systems involving Monte Carlo methods adopted temperature convergence [10] [26].

The flux (and therefore power) uncertainty from Monte Carlo method is propagated through the thermal-hydraulics parameters, such as temperature. In the previous publications, the convergence criterion was set by monitoring the peak temperature, such that it was within the pre-set tolerance limit [10]. However, this does not prove global convergence, only local convergence, because the temperature error should be monitored at every axial node.

It is already shown that by using local axial power as the convergence criterion, the UO2 single assembly model converges at step 7 and MOX single assembly model converges at step 10. In order to prove convergence, thermal-hydraulics parameters like coolant mass density, fuel, coolant and clad temperatures, should be converged, too. Because coolant temperature converges earlier than the fuel temperature [26], only the coolant mass density, fuel and clad temperatures are checked.

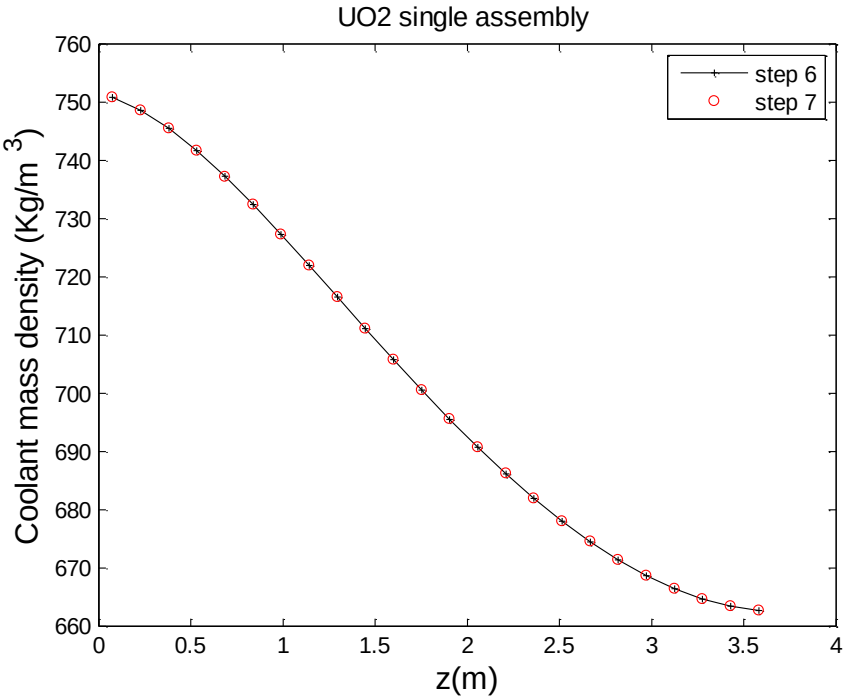

Figure 6.3: Convergence of coolant mass density for UO2 models

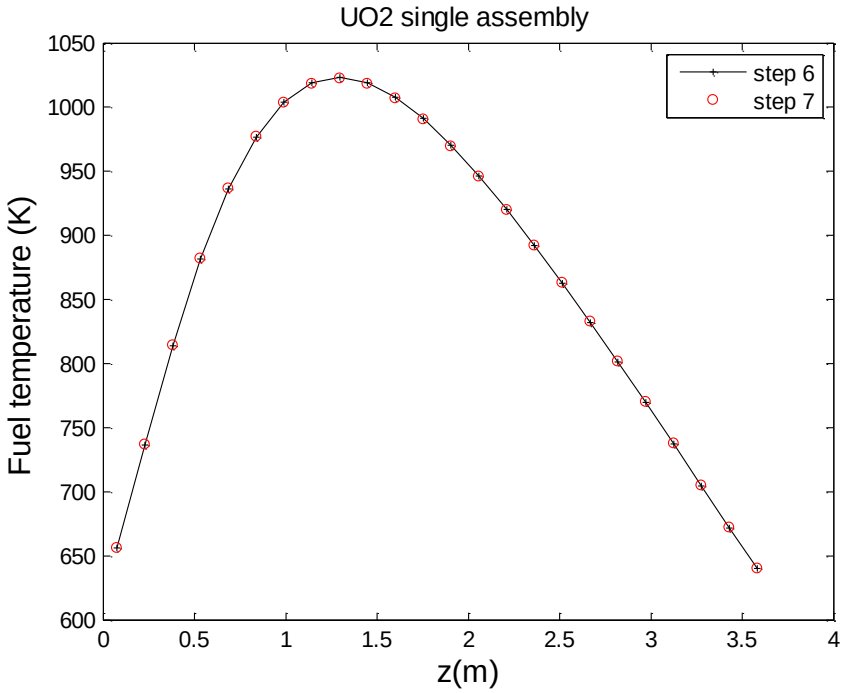

Figure 6.4: Convergence of fuel temperature for UO2 models

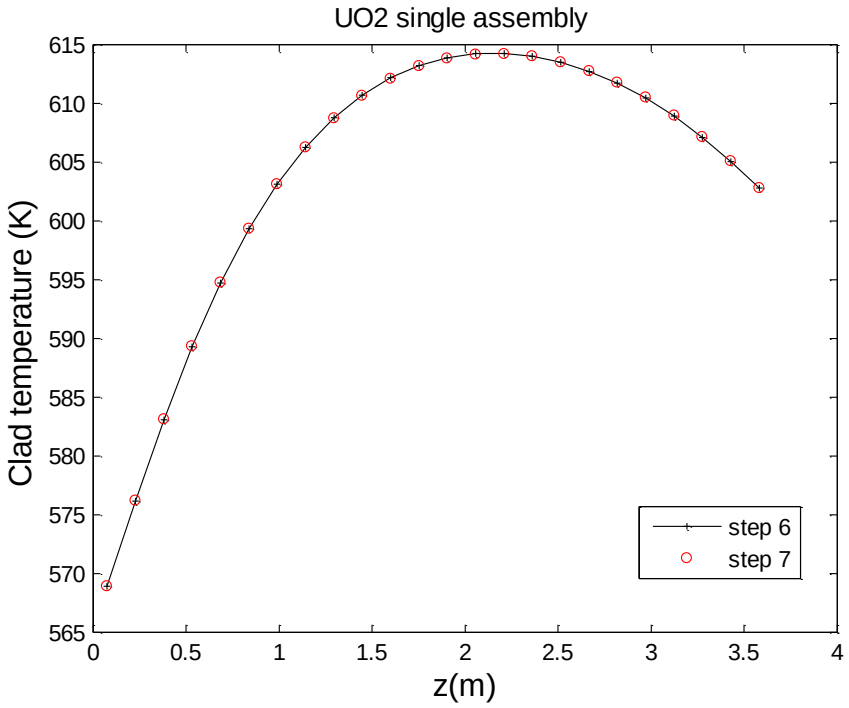

Figure 6.5: Convergence of clad temperature for UO2 models

Based on the comparison of thermal-hydraulics parameters between coupling step 6 and step 7 for the UO2 single assembly model, it is obvious that these parameters are converged. The maximum relative error is 0.003% for coolant mass density, 0.094% for fuel temperature and 0.010% for clad temperature. The fuel temperature and the axial power distribution share a similar shape.

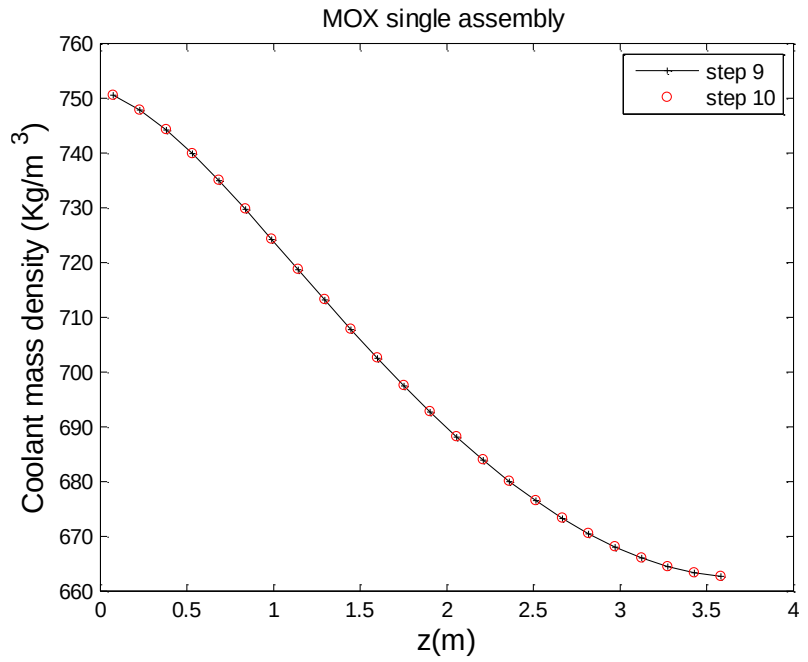

Figure 6.6: Convergence of coolant mass density for MOX models

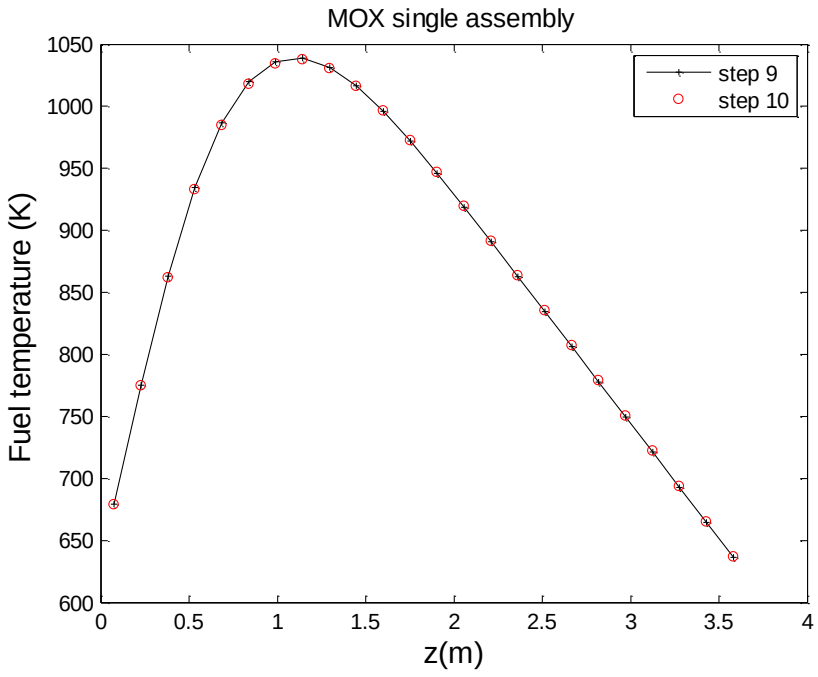

Figure 6.7: Convergence of fuel temperature for MOX models

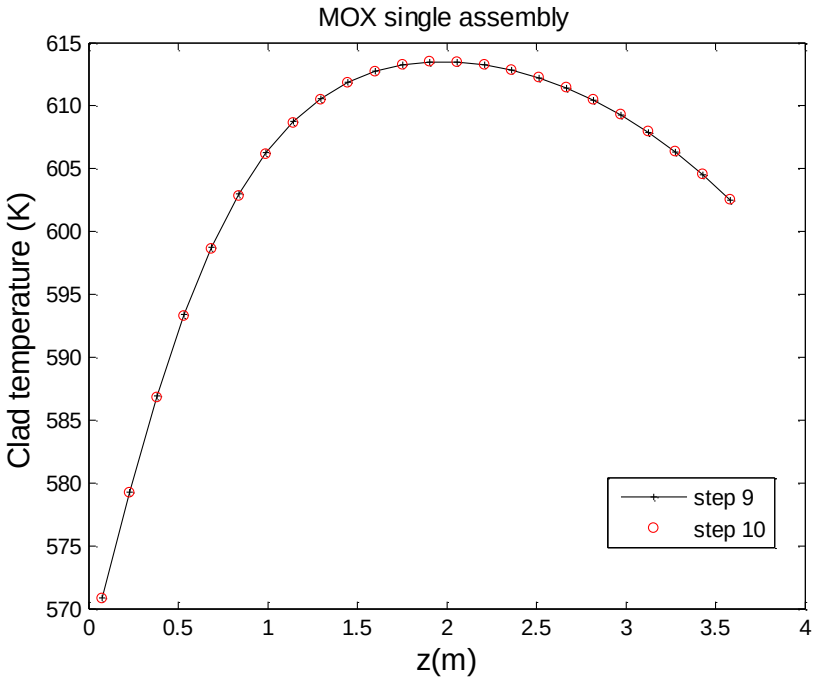

Figure 6.8: Convergence of clad temperature for MOX models

Similar to the UO2 single assembly case, the three considered thermal-hydraulics parameters (coolant density, fuel temperature, cladding temperature) are also well converged for the MOX single assembly. The maximum relative error is 0.019% for coolant mass density, 0.206% for fuel temperature and 0.025% for clad temperature.

The convergence criteria used by previous researchers [10] [26] is relative temperature error of 0.6% ~ 1%. This is higher than the maximum relative error achieved in this thesis. This shows that the axial power converges later than the thermal-hydraulics parameters [26]. Therefore, the axial power distribution convergence criteria adopted in this thesis is not only easier and more direct, but also more rigorous.

6.3 Coupling results

The comparison of coupled Serpent/RELAP5-3D and DeCART multiplication factor is shown in Table 6.1. Compared with results in Table 5.3, the difference is significantly smaller when thermal-hydraulics feedback is used. The most likely reason is the cancelation of error between the neutronics solution and the thermal-hydraulics solvers in DeCART and RELAP5-3D.

Table 6.1: Multiplication factor comparison of Serpent/RELAP5 and DeCART

Multiplication Factor			
	DeCART, with thermal-hydraulics feedback	Serpent/RELAP5-3D	Difference (pcm)
UO2_3D	1.41148	1.41367	219
MOX_3D	1.32713	1.33083	370

((Note that every eigenvalue in Table 6.1 by Serpent has a statistical error of 1.3E-05.)

The normalized axial power distribution comparison is shown on Figure 6.9 and 6.10 for UO2 and MOX assembly, respectively.

Figure 6.9 includes normalized axial power distribution from Serpent and DeCART without thermal-hydraulics feedback. The figure shows that the axial power distribution is considerably shifted when thermal-hydraulics feedback is introduced. The coupled Serpent/RELAP5-3D results are consistent with DeCART results with feedback, especially when error bar is taken into consideration.

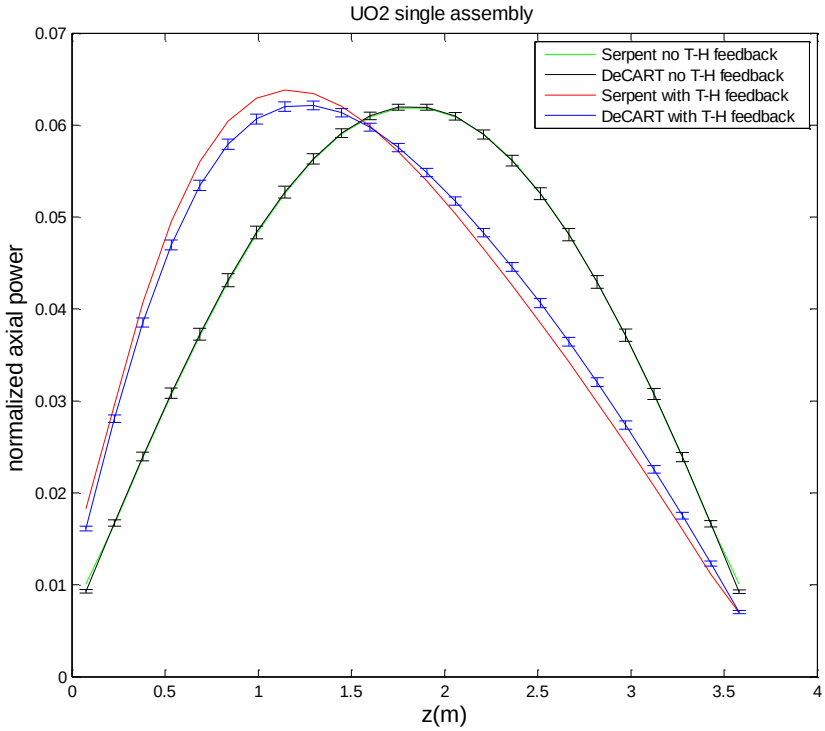

Figure 6.9: Axial power distribution, UO2 model

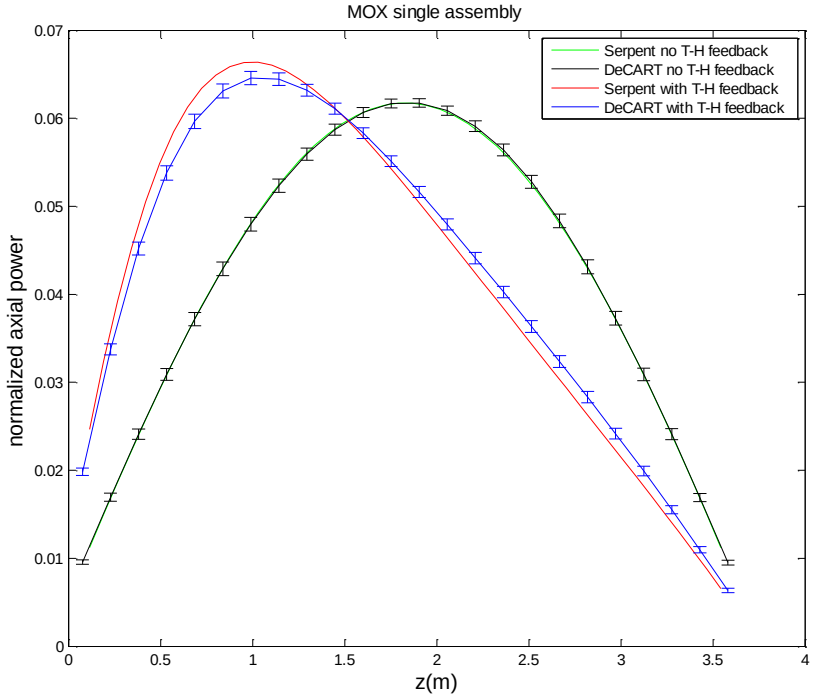

Figure 6.10: Axial power distribution, MOX model

The MOX single assembly model shows the same behavior as the UO2 single assembly model. Therefore, it can be concluded that the coupling of Serpent with RELAP-3D does converge in only a few steps, and the coupling results are well verified by the DeCART code.

CHAPTER 7. CONCLUSIONS AND FUTURE PLANS

In this thesis, a three-dimensional continuous-energy Monte Carlo reactor physics code, Serpent was coupled with the thermal-hydraulics safety analysis code RELAP5-3D. This coupling is intended to improve the prediction capability and applicability of the codes for reactor safety applications. The coupling method was tested with the OECD-NEA/NRC PWR MOX-UO2 Core Transient Benchmark, and the DeCART code was used to verify the coupling.

A new convergence criterion based on the normalized axial power distribution was introduced. The new criterion considers the inherent feature of Monte Carlo methods and uses the statistical uncertainty of the normalized axial power distribution. This convergence criterion is shown to be more direct, easier to apply and more rigorous than the temperature convergence used in previous research.

The coupling of Serpent and RELAP5-3D codes was shown to converge in a few steps for both UO2 and MOX single assembly models. The results were verified by the corresponding DeCART results. Both the multiplication factor and normalized axial power distribution were in a very good agreement. The results in this thesis have shown that Serpent can be coupled with deterministic thermal-hydraulics codes.

DeCART is adopted as the verification code for the coupling for that it has internal thermal-hydraulics feedback module. But as can be seen in section 5.3, the difference in multiplication factor between DeCART and Serpent is too large, especially for the 3-D

cases. In the future, other Monte Carlo codes or system thermal-hydraulics codes will be used to verify the coupling between Serpent and RELAP5-3D.

Additionally, the future work will be to adopt additional physics into the coupling, e.g. chemistry and thermal mechanical effects, in addition to reactor physics and thermal-hydraulics. Recent research [6] has successfully incorporated crud chemistry into the coupling of full-core neutron transport code DeCART and Computational Fluid Dynamics code STAR-CCM+, where the MAMBA code was used as the macro-scale coolant chemistry code and crud deposition code. This coupling of three independent physics is an example of advanced high-fidelity simulation, which should be still expanded, refined and improved to further the understanding of nuclear reactor technology multi-physics effects.

REFERENCES

[1] Kozlowski, T. and Downar, T. J. "OECD/NEA and US NRC PWR MOX/UO2 Core Transient Benchmark." Working Party of the Physics of Plutonium Fuels and Innovative Fuel Cycles, OECD/NEA Nuclear Science Committee, 2003.

[2] Kozlowski, T. et al. "Analysis of the OECD MSLB Benchmark with the Coupled Neutronics and Thermal-Hydraulics Code RELAP5/PARCS." *Proceedings of Advances in Reactor Physics, and Mathematics and Computation into the Next Millennium (PHYSOR-2000),* Pittsburgh, Pennsylvania, May 7-11, 2000.

[3] Hu, Y., Downar, T. J., Kozlowski, T., Ivanov, K., Staudenmeier, J. "Multi-physics coupled code reactor analysis with the US NRC code system TRACE/PARCS". *Proceedings of PHYSOR-2006,* CD-ROM (Electronic Publication), Vancouver, Canada, 2006.

[4] Xi, X., et al. "The axial power distribution validation of the SCWR fuel assembly with coupled neutronics-thermal-hydraulics method." Nuclear Engineering and Design 258 (2013): 157-163.

[5] Ivanov, K., and Maria A. "Challenges in coupled thermal–hydraulics and neutronics simulations for LWR safety analysis." Annals of Nuclear Energy 34.6 (2007): 501-513.

[6] Walter, D., et al. "High Fidelity Simulation of Crud Deposition on a PWR Fuel Cell with Spacer Grids over a 500 Day Depletion Cycle". *Proceedings of the 15th International Topical Meeting on Nuclear Reactor Thermal-hydraulics (NURETH-15),* Pisa, Italy, May 12-15, 2013.

[7] X-5 Monte Carlo Team, "MCNP - A General Monte Carlo N-Particle Transport Code, Version 5", Los Alamos National Laboratory, 2003.

[8] Leppänen, J. “Development of a New Monte Carlo reactor physics code.” Ph.D. Thesis, VTT Technical Research Centre of Finland, 2007.

[9] Smith, K., "Spatial Homogenization Methods for Light Water Reactor Analysis." Ph.D. Thesis, Massachusetts Institute of Technology, 1980.

[10] Vazquez, M., et al. "Coupled neutronics thermal-hydraulics analysis using Monte Carlo and sub-channel codes." Nuclear Engineering and Design 250 (2012), 403-411.

[11] Breitkreutz, H., Röhrmoser, A. and Petry, W. "3-Dimensional Coupled Neutronics and Thermal-Hydraulic Calculations for a Compact Core Combining MCNPX and CFX." Nuclear Science, IEEE Transactions on 57.6 (2010): 3667-3671.

[12] Serker, V., Thomas, J. W. and Downar, T. J. "Reactor physics simulations with coupled Monte Carlo calculation and computational fluid dynamics." *Proceedings of Joint International Topical Meeting on Mathematics and Computation (ICENES-2007)*, Istanbul, Turkey, June 3-8, 2007.

[13] Weber, D. P. et al, "Coupled Calculations Using the Numerical Nuclear Reactor for Integrated Simulation of Neutronics and Thermal-Hydraulic Phenomena", *Proceedings of the PHYSOR 2004*, Chicago, IL, April 2004.

[14] Kotlyar, D., et al. "Coupled neutronics thermo-hydraulic analysis of full PWR core with Monte-Carlo based BGCore system." Nuclear Engineering and Design 241.9 (2011), 3777-3786.

[15] Leppänen, J. "Serpent–a Continuous-energy Monte Carlo Reactor Physics Burnup Calculation Code". User's Manual, VTT Technical Research Centre of Finland, Espoo, Finland, 2012.

[16] The RELAP5-3D Development Team, "RELAP5-3D Code Manual, Volume 1: Code Structure, System Models and Solution Methods". Idaho National Engineering and Environmental Laboratory, INEEL-EXT-98-00834, Revision 4.0, 2012.

[17] Joo, H. G., et al. "Methods and performance of a three-dimensional whole-core transport code DeCART." *Proceedings of the PHYSOR 2004*, pp. 21-34, Chicago, IL, April 2004.

[18] Leppänen, J. "A new assembly-level Monte Carlo neutron transport code for reactor physics calculations." Mathematics and Computation, Supercomputing, Reactor Physics and Nuclear and Biological Applications, American Nuclear Society, LaGrange Park, IL, 2005.

[19] Leppänen, J. "Performance of Woodcock delta-tracking in lattice physics applications using the Serpent Monte Carlo reactor physics burnup calculation code." Annals of Nuclear Energy 37.5 (2010): 715-722.

[20] Leppänen, J. "Two practical methods for unionized energy grid construction in continuous-energy Monte Carlo neutron transport calculation." Annals of Nuclear Energy 36.7 (2009): 878-885.

[21] Kochunas, B., Hursin, M. and Downar, T. J. "DeCART v2.05 User's Manual", School of Nuclear Engineering and Radiological Sciences, University of Michigan, 2009.

[22] Finnemann, H., and Galati, A. “NEACRP 3-D LWR Core Transient Benchmark: Final Specifications”. 1992.

[23] MacFarlane, R. E. and Muir, D. W. “NJOY99.0 Code System for Producing Point-wise and Multi-group Neutron and Photon Cross Sections from ENDF/B Data”, PSR-480, Los Alamos National Laboratory (2000).

[24] Brown, F.B., Martin, W.R., Yesilyurt, G., Wilderman, S., “Progress with On-The-Fly Neutron Doppler Broadening in MCNP”. Transactions of the American Nuclear Society, p. 106, 2012.

[25] Herman, M., Trkov, A., “ENDF-6 Formats Manual-Data Formats and Procedures for the Evaluated Nuclear Data Files ENDF/B-VI and ENDF/B-VII”. Brookhaven National Laboratory, BNL-90365-2009.

[26] Sanchez, V., and Al-Hamry, A. "Development of a coupling scheme between MCNP and COBRA-TF for the prediction of the pin power of a PWR fuel assembly." *Proceedings of International Conference on Mathematics, Computational Methods & Reactor Physics*. Saratoga Springs, New York, May 3-7, 2009.